

Effects of the Chemical Composition of Synthetic Slags Compared to an Average Blast Furnace Slag

Luis Schnürer¹ | Alisa Machner¹

Correspondence

Luis Schnürer, M.Sc.
Technical University of Munich
TUM School of
Engineering and Design
Department for
Materials Engineering
cbm Centre for Building Materials
Professorship for Mineral
Construction Materials
Franz-Langinger-Str. 10
81245 Munich – Germany
Email: luis.schnuerer@tum.de

¹ Technical University of Munich,
Germany

Abstract

To study the effect of the main oxides and the minor components in slags on their reactivity as SCM, various glasses were synthesized to stepwise imitate a commercial slag of average chemical composition. First, a glass was produced from the main oxides CaO, Al₂O₃ and SiO₂. In a second step, the minor components MgO, Fe₂O₃, Na₂O and K₂O were added separately to the main oxide mix. A selection of two synthetic glasses was tested for their compressive strength contribution (up to 90 days) by substituting 20 wt.% of cement. After all testing times, the synthetic slags achieved a strength similar to that of the commercial product. The reactivities determined by heat flow calorimetry (R³ test) correlate with the calculation of NBO/T and the results of ²⁹Si MAS NMR showing that a decreased degree of polymerization enhances the reactivity. Apart from that, FTIR spectroscopy and ²⁷Al MAS NMR indicate a similar structure of the original and the synthetic slags.

Keywords

Synthetic Glasses, SCMs, Compressive Strength, Reactivity, Structure

1 Introduction

In 2022, roughly 4.1 billion tons of cement were produced globally [1], which makes it worldwide the most produced and used material [2]. Since cement production is an energy intensive manufacturing process and requires the calcination of limestone, this procedure accounts for around 7 % of the global industrial energy used [3] and for up to 8 % of the anthropogenic CO₂ emissions [4]. One common strategy to limit the total emissions from cement production is substituting the clinker in cements by SCMs like blast furnace slags [5].

Such blast furnace slags are a by-product in the pig iron production process. Rapid cooling of the molten slags with air or water results in a largely amorphous material consisting mainly of Al₂O₃, SiO₂, CaO and MgO [6,7], where Al₂O₃, SiO₂ and CaO represent also the main components of cement, which makes it a suitable SCM due to containing the same reactive components like cement [8]. Slags have higher CaO content compared to pozzolans but still lower than that of cement [9]. Therefore, they are mainly latent-hydraulic. For their hydration, the pH of the pore solution has to be kept high enough by activators – like alkali hydroxides or portlandite [10,11] – to continuously dissolve the slag [8]. Due to a higher Al₂O₃ content in slags compared to cement, aluminum replaces parts of the silicon in C-S-H to form C-A-S-H phases [12,13]. C-A-S-H phases formed by the slag reaction have a lower Ca/Si ra-

tio compared to the C-S-H from cement hydration [8]. Additionally, AFm phases and hydrotalcite are formed [8,14–16]. The hydration of slags is slower but continues longer than that of cement. Therefore, a denser microstructure is formed in cements blended with slag [17]. Especially the reaction of finer slag particles leads to pore refinement and lower capillary porosity and thus to greater durability properties [18].

The chemical composition has a huge effect on the reactivity and overall reaction of slags [19]. Type and quantity of occurring main oxides vary depending on the raw materials used and process conditions during the formation [6,10]. Due to the different and complex composition of slags, it is difficult to study the effect of individual components on the reactivity. We want to investigate these effects by investigating slags with a simplified composition. Synthetic glasses are a simple solution to reduce the number of oxides in slags by excluding different components, which are normally found in slags to consider only selected compositions. If ground to a similar specific surface area, a comparison of different slag compositions is possible with regard to the effects of different oxides, e.g. on the reactivity in the slag.

In addition, our study aims to show how realistic synthetic glasses are to mimic commercial slags. We have therefore synthesized different glasses that are modelled on the oxide ratios of a commercial slag, but differ in the type and amount of oxides, and compared their compressive

strength in mortars. The compressive strength was then correlated with their reactivity resulting from their structure.

2 Experimental

2.1 Materials

We prepared five variations of an original blast furnace slag (OS). The synthesis was aligned to as described in [20]. First, a basic mix (BS) containing only the main oxides Al_2O_3 , SiO_2 and CaO was prepared. Then, we mixed these main oxides with Fe_2O_3 (FS), MgO (MS), the alkali oxides Na_2O and K_2O (AS) or with all of them to a more realistic mix (RS). The weight ratio of the included oxides should be equal to OS. For the synthesis, CaO , Na_2O and K_2O were used as the corresponding carbonate. Therefore, all mixes were interground in portions corresponding to 60 g of glass using a mortar mill (3 cycle; 3 min each) and calcined in a Pt crucible for 16 h at 1000 °C. After cooling, we ground all mixes in the mortar mill (1 cycle; 3 min), filled them in the Pt crucibles again and melted them for 2 h at 1500 °C. The crucibles were removed from the furnace at 1500 °C and the resulting glass melt was quenched in air. The glassy material was ground to a specific surface area (Blaine) of approx. 4400 g/cm^2 corresponding to OS using a vibratory disc mill made of stainless steel. Their Blaine value is shown next to the specific surface area determined by BET and their density determined by He pycnometry in Table 1. Their particle size distribution was measured by laser diffraction and is presented in Figure 1. Table 2 states their corresponding d_{10} , d_{50} and d_{90} values.

Table 1 Physical properties of the original (OS) and synthetic slags (RS, BS, FS, MS and AS)

Short name	Blaine [cm^2/g]	BET [cm^2/g]	Density [g/cm^3]
OS	4402	11479	2.91
RS	4382	10080	2.93
BS	4366	8370	2.90
FS	4555	9174	2.90
MS	4400	8793	2.93
AS	4394	7783	2.88

The original slag (OS) used was supplied by Märker, the cement CEM I 42.5 R (CEM) for the compressive strength tests was supplied by HeidelbergCement and the limestone powder *Wiesenhofen* (LS) used as a reference was supplied by Max Bögl. The chemical composition of cement, limestone, original slag (Table 3) and synthetic slags (Table 4) were determined by ICP-OES. QXRD was used to identify the mineralogical composition of all slags. OS was used as received from the manufacturer and was 86.0 wt.% amorphous and contained 0.3 wt.% quartz and 3.0 wt.% åkermanite in addition to 4.3 wt.% alite, 1.5 wt.% ferrite, 2.0 wt.% gypsum and 2.9 wt.% bas-

sanite. The amounts of clinker and gypsum and the relatively low amorphous content indicate that something was added to the blast furnace slag. Therefore OS is not to be regarded as average blast furnace slag. BS, FS and AS were completely amorphous, while RS (3.2 wt.%) and MS (2.5 wt.%) contained small amounts of merwinite.

Table 2 d_{10} , d_{50} and d_{90} [μm] of the original (OS) and synthetic slags (RS, BS, FS, MS and AS)

Short name	d_{10} [μm]	d_{50} [μm]	d_{90} [μm]
OS	2.79	12.52	32.74
RS	2.00	12.49	49.84
BS	2.05	10.38	47.18
FS	1.91	8.61	35.26
MS	2.16	13.93	53.93
AS	2.16	10.00	40.16

2.2 Methods

2.2.1 Compressive strength test

For the determination of compressive strength, binder blends consisting of 20 wt.% OS, RS or BS and 80 wt.% CEM were produced.

Mortars prepared with pure OPC and blends containing limestone powder (20 wt.%) served as references. Compressive strengths were tested at 7, 28 and 90 days to examine strength development. The mortars were prepared and cured according to DIN EN 196-1 [21]: The mortars were prepared by mixing binder, standard sand and water in a weight ratio of 1:3:0.5, cast into molds (40 mm x 40 mm x 160 mm) and stored at 20 °C and 95 % rel. h. for 1 day. After 1 day, the mortar bars were demolded and stored under water at 20 °C until the day of testing was reached. At each testing date, 3 mortar bars per sample were split in two and each half was tested for their compressive strength that a total of 6 compressive strength values per sample type and age were gained and tested.

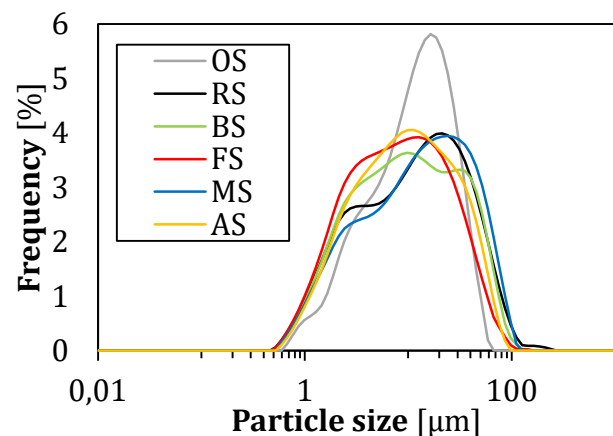


Figure 1 Particle size distribution of the original (OS) and synthetic slags (RS, BS, FS, MS and AS), determined by laser diffraction

Table 3 ICP-OES results [wt.%] of the cement (CEM), limestone (LS) and the original slag (OS)

Oxide	CEM	LS	OS
Al ₂ O ₃	5.03	0.04	11.04
SiO ₂	20.09	0.06	34.29
CaO	64.35	52.45	37.28
Na ₂ O	0.19	0.13	0.47
K ₂ O	0.57	0.12	1.26
MgO	1.54	0.80	10.00
Fe ₂ O ₃	3.20	0.10	0.77
SO ₃	3.13	0.14	4.10
LOI	2.20	42.58	0.46
sum	100.30	96.42	99.67

2.2.2 R³ test

For the estimation of the SCM reactivity, isothermal heat flow calorimetry was performed in a model system at 40 °C. The measurement was conducted in a *TAM Air 8*-channel isothermal calorimeter. Instead of using OPC blended with the SCMs, a system made of portlandite, SCM and calcite was used and mixed with a solution containing potassium sulfate and potassium hydroxide. This test is referred as "R³ test" in the literature [22]. The method was applied for OS, RS, BS, MS, FS, AS and LS. The ratio of these chemicals is specified in ASTM C1897-20 standard [23]: Three times the amount of portlandite and half the amount of calcite relative to the SCM were blended.

Table 4 ICP-OES results [wt.%] of the various synthetic slags (RS, BS, MS, FS and AS)

Oxide	RS	BS	FS	MS	AS
Al ₂ O ₃	11.67	13.55	13.49	12.44	13.24
SiO ₂	34.96	40.22	40.31	36.32	39.88
CaO	39.23	45.72	44.54	39.82	43.90
Na ₂ O	0.53	0.09	0.05	0.11	0.64
K ₂ O	1.38	0.28	0.15	0.29	1.73
MgO	10.26	0.28	0.12	10.87	0.12
Fe ₂ O ₃	0.90	0.04	1.04	0.03	0.03
SO ₃	0.10	0.10	0.05	0.03	0.08
LOI	0.39	0.34	0.36	0.29	0.28
sum	100.62	99.90	100.11	100.20	99.42

The potassium solution was prepared by dissolving 4.0 g potassium hydroxide and 20.0 g potassium sulfate in 1 L deionized water. All chemicals were heated to 40 °C before mixing and the calorimeter temperature was adjusted also to 40 °C. The dry mix (6.8182 g) was placed into a glass ampoule and the potassium solution (8.1818 g) was added, mixed thoroughly for 2 min and placed inside the calorimeter subsequently. The total heat was then recorded for 7 d.

2.2.3 FTIR spectroscopy

The slag structure was analyzed by Fourier-transformed infrared (FTIR) spectroscopy. A FTIR spectrometer *Spectrum 100* (Perkin Elmer) with a Golden Gate Diamond ATR unit was used and the transmittance was measured between the wavenumbers 450 and 4000 cm⁻¹ with a step width of 1 cm⁻¹.

2.2.4 ²⁷Al and ²⁹Si MAS NMR

Another method to characterize the structure of the slags is ²⁷Al and ²⁹Si MAS NMR. The spectra were recorded by a *Bruker Avance 300* spectrometer (magnetic field strength 7.0455 T, resonance frequency of ²⁷Al: 78.12 MHz and ²⁹Si: 59.63 MHz). The slags were packed in 4 mm zirconia rotors for the ²⁷Al (spinning rate: 15 kHz) and in 7 mm zirconia rotors for ²⁹Si NMR measurements (spinning rate: 5 kHz) and were spun at the magic angle (MAS). For the ²⁷Al measurements 2000 scans were taken with a repetition time of 0.5 s and the chemical shifts were set relative to aluminum hydroxide. The ²⁹Si spectra were recorded with a repetition time of 45 s and over 2000 scans were taken. The chemical shifts were recorded relative to tetramethylsilane. ²⁷Al and ²⁹Si MAS NMR experiments were performed with single pulse technique.

3 Results & discussion

The compressive strength was determined for the slags OS, RS, BS and for the references LS and CEM after 7, 28 and 90 days. The results are shown in Figure 2.

After 7 d, the compressive strength of all mortars blended with SCMs are relatively similar ranging from 39.9 (BS) to 43.8 N/mm² (RS). That is true even for the inert LS. This is consistent with the findings of *Lawrence et al.* [24]. For early hydration times, the compressive strength is independent of the nature of the SCM and depends only on the specific surface area of the SCM. The CEM reference, which contains only cement, has a significantly higher compressive strength than the blended cements, reaching a compressive strength of 53.0 N/mm².

After 28 d, however, pronounced differences between the blended systems are detectable. LS has the lowest (49.5 N/mm²) and RS the highest compressive strength (64.3 N/mm²), even higher than CEM (62.4 N/mm²). The compressive strength of OS (59.2 N/mm²) and BS (59.0 N/mm²) is almost the same.

As after 28 d, mixtures with 20 wt.% LS have the lowest compressive strength at 55.7 N/mm² after 90 d. The compressive strengths of CEM, OS, RS and BS are in a similar

range between 71.4 (RS) and 75.4 N/mm² (OS). In contrast to the values after 28d, those of RS are no longer above OS and BS, but just below. Overall, it can be said that the compressive strengths of the synthetic slags RS and BS and the original slag OS provide comparable values after 7, 28 and 90 d, which deviate from one another by no more than 10%.

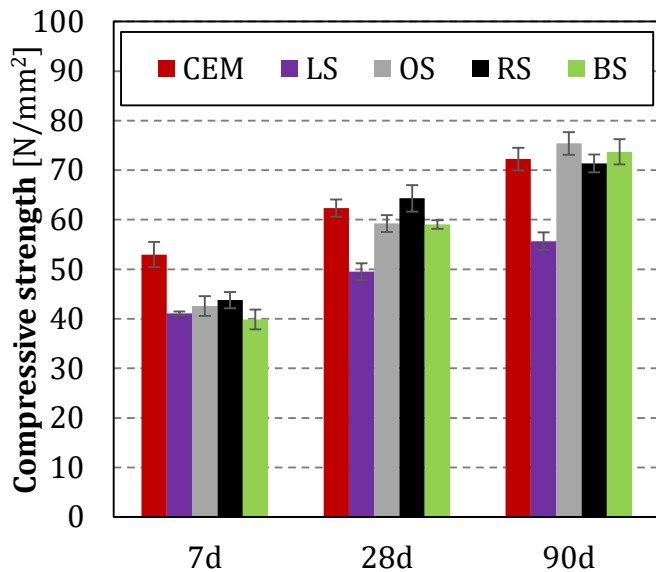


Figure 2 Compressive strength of CEM I 42.5 R and blends with 20 wt.% LS, OS, RS and BS after 7, 28 and 90 days with error bars according the statistical standard deviation

Since limestone is an inert SCM, it is expected that LS has the lowest compressive strength after 28 and more days contributing only due to the “filler effect” [25], which includes effects of dilution and heterogeneous nucleation [26–28]. However, the slag reaction leads in addition to the filler effect to increased strength. Due to the similarity in specific surface area (Table 1), differences between the slags due to physical effects should be negligible and be attributed to the different reactivities resulting from the chemical and mineralogical composition.

One method to estimate the reactivity of SCMs is to determine the cumulative total heat of an SCM with isothermal heat flow calorimetry in an environment, which mimics hydrating cement (R³ test). The heat of hydration of LS, OS, RS and BS are shown next to FS, MS and AS for 7 d in Figure 3. For a better overview, the values of the total heat after 1, 3 and 7 d are shown in Table 5.

The cumulative heats of the tested SCMs proceed in different ways. Limestone is inert and does not generate a significant amount of heat. In contrast, the original and synthetic slags show a steep increase in heat over the first 12 to 24 h. While BS, FS and AS have a total heat of approx. 250 – 260 J/g SCM after 3 d (72 h) and 310 – 330 J/g SCM after 7 d (168 h), RS and MS achieve higher heat in this period (3 d: ~330 J/g SCM; 7d: ~390 J/g SCM). OS has a lower total heat than RS and MS from start of the measurement to 30 h. Then, the total heat of OS surpasses that of RS and MS and shows overall the highest total heat after 7 d with a difference of about 80 J/g SCM.

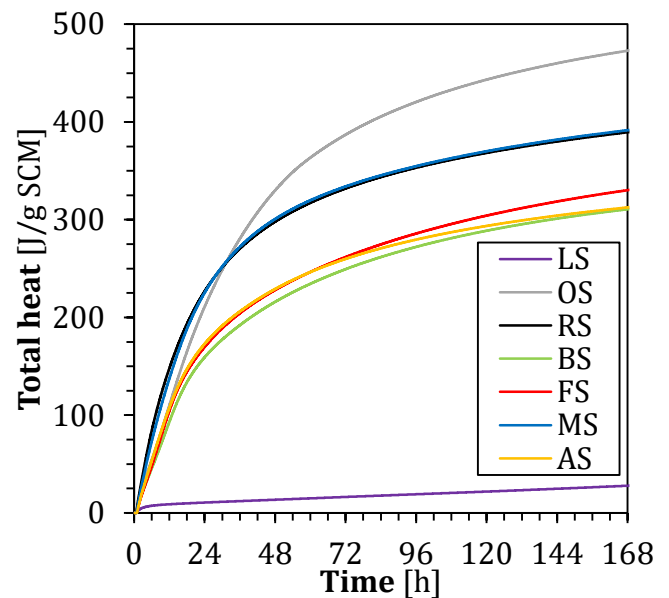


Figure 3 Cumulative total heat of LS, OS, RS, BS, FS, MS and AS for 7 days at 40 °C in the R³ test

Table 5 Total heat of all SCMs in the R³ test after 12, 72 and 168 h

Short name	Total Heat [J/g SCM]		
	12 h	72 h	168 d
LS	8.9	16.4	27.8
OS	110.2	387.0	472.9
RS	148.4	332.0	389.5
BS	94.7	249.6	310.7
MS	139.1	334.2	391.6
FS	106.4	262.0	330.3
AS	110.0	260.2	312.7

According to *Li et al.* [29], the total heat determined in the R³ test after 12 or 24 h correlates with the compressive strength after 7 d and the total heat after 7 d with the compressive strength after 28 d. That is true for the compressive strength of OS, RS and BS after 7 d, since the series for total heat after 12 or 24 h and compressive strength after 7 d from highest to lowest is the same: RS > OS > BS. However, LS must be excluded as it has comparable compressive strength to BS after 7 d but the total heat is significantly lower since LS produces only a small amount of heat. A correlation between strength after 28 d and total heat after 7 d cannot be observed. Although there is a correlation for BS and RS, this does not apply to OS. BS produces lower total heat and has lower compressive strength. In contrast, OS has by far the highest total heat, but a compressive strength after 28 d comparable to that of BS. *Blotevogel et al.* [30] showed in their research that total heat and compressive strength correlate well only in the first 2 d and with ongoing time the correlation decreases, what is observed for OS, RS and BS after 7 d.

For reactivity of SCMs, the degree of polymerization is considered to be an important factor [31]. Therefore, the ratio of non-bridging oxygen to tetrahedral oxygen (NBO/T) is calculated from the chemical composition of the amorphous contents from all slags according to eq. 1 from *Senior and Srinivasashar* [32]. The ratio is ranging from 0, where all oxygen atoms are tetrahedrally coordinated to central atoms (e.g. in a pure silicate network), to 4, where no network can be formed as there are only non-bridging oxygen atoms [33].

$$NBO/T = (\sum x_{M_2O} + \sum x_{MO} - \sum x_{M_2O_3}) / (\sum x_{MO_2}/2 + \sum x_{M_2O_3}) \quad (1)$$

where x is the mole fraction of a certain oxide and M_2O stands for Na_2O and K_2O , MO for CaO and MgO , MO_2 for SiO_2 and M_2O_3 for Al_2O_3 and Fe_2O_3 . The NBO/T ratio is calculated according to this equation for composition of the amorphous part of the original and the synthetic slags and the results are shown in Table 6.

Table 6 degree of polymerization (NBO/T) for the original (OS) and the synthetic slags (RS, BS, FS, MS and AS)

	OS	RS	BS	MS	FS	AS
NBO/T	2.04	2.24	1.69	2.19	1.59	1.68

The higher the NBO/T ratio, the more oxygen atoms are non-bridging and thus terminal atoms. This means that these compounds are not highly polymerized. In contrast, a structure with a lower NBO/T ratio has more bridging oxygen atoms and is therefore more highly polymerized since it has fewer non-bridging oxygen atoms.

The OS, RS and MS have a similar degree of polymerization coming mainly from the MgO in comparison to BS, FS and AS (Table 3 and Table 4). Due to the high amount of MgO in the slag (~10 wt.%), which is a network modifier, the silicate basic structure is increasingly depolymerized. That can be seen by the increased number of non-bridging oxygen (NBO), which leads to faster hydrolysis and thus to an increased rate of dissolution [34]. A faster dissolution ultimately leads to faster reaction, since only dissolved substances can react to form reaction products.

The NBO/T ratios of the slags tested correlate well with the heat development in the heat flow calorimetry. A lower degree of polymerization results in higher total heat and therefore increased reactivity. OS, RS and MS have a clearly higher NBO/T and total heat value after 7 d than the other slags. BS, FS and AS have relatively similar regarding NBO/T values and total heat after 7 d. Overall, a clear relationship between the degree of polymerization and the reactivity is recognizable.

This ratio is a theoretical calculation in order to be able to make initial statements about the structure of the slags and their differences. In order to be able to identify further similarities and differences in the structure, the slags were also examined experimentally. One of the methods used was FTIR spectroscopy.

The FTIR spectra show no absorption bands in the wave-number range from 4000 – 1500 cm^{-1} for the original and

all synthetic slags. Therefore, only the range from 1500 – 450 cm^{-1} is shown in Figure 4.

In all spectra, absorption bands can be seen at wave-numbers of 906 and 689 cm^{-1} , with the band at 906 cm^{-1} being due to Si-O-T/T-O-Si stretching vibrations and the band at 689 cm^{-1} being due to Si-O-T bending vibrations, where T stands for either Si or Al [35]. In this way, aluminosilicates can be clearly detected. For OS there is an additional band at 1150 cm^{-1} . This is due to u_3 vibration of the sulfate ion [36], which is found only in OS in the form of gypsum and bassanite. But apart from that difference, there are no structural differences recognizable. This indicates a similar structure of the different slags.

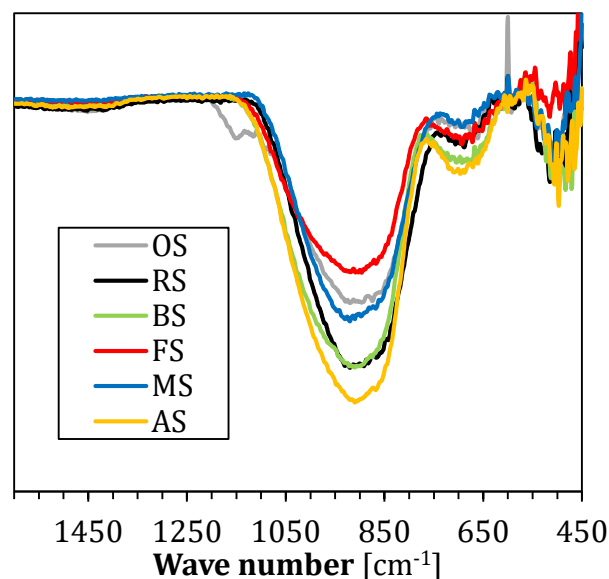


Figure 4 FTIR spectra of the original (OS) and synthetic slags (RS, BS, FS, MS and AS)

Figure 5 shows the 1D ^{27}Al MAS NMR spectra of OS and the synthetic slags. The OS has by far the lowest signal intensity. The chemical shifts of the single peaks of all slags suggest that aluminum is mainly fourfold coordinated. The asymmetrical appearance of the peaks indicates that fivefold coordinated aluminum is also present. Due to the broadening of second order quadrupolar interaction, it is not possible to quantify both species. According to the literature, the total proportion of fivefold coordinated aluminum in glasses of a similar composition should not be greater than 7 wt.% [37,38].

The ^{29}Si MAS spectra of the different slags are shown in Figure 6. Again, all spectra exhibit just one single broad peak and OS has the lowest signal of all peaks. Due to the fact that the peaks are relatively broad (approx. 30 ppm) and cover a range between -50 and -100 ppm each, Q^1 and Q^2 can be identified [37,39]. OS, RS and MS have located their center of gravity between -70.5 and -75.2 ppm and BS, FS and AS have theirs around -78 ppm indicating a upfield shift and a higher polymerization [40]. That means that they exhibit a higher amount of Q^2 compared to the other slags and a lower amount of Q^1 . That can also be seen in the calculated NBO/T (Table 6). Clearly, a decreased degree of polymerization leads to a higher number of lesser linked silicates (Q^1 in this case), which increases the NBO/T ratio and thus the reactivity determined by the

R³ test. This trend can also be seen in the compressive strengths of mortars prepared with the synthetic slags after 28 days. Since a higher degree of polymerization in the glasses results in lower strength of mortar samples prepared with them.

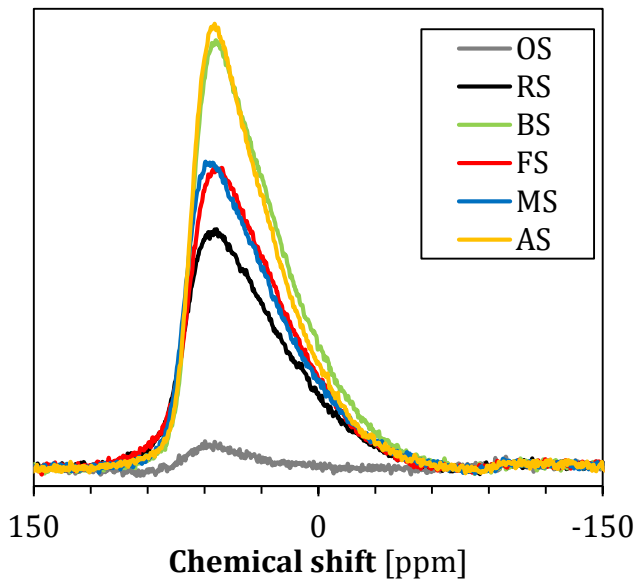


Figure 5 ²⁷Al MAS NMR spectra of the original (OS) and synthetic slags (RS, BS, FS, MS and AS)

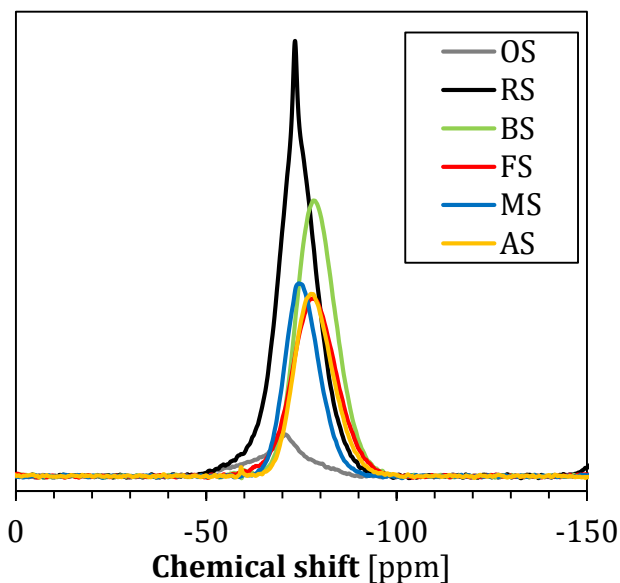


Figure 6 ²⁹Si MAS NMR spectra of the original (OS) and synthetic slags (RS, BS, FS, MS and AS)

4 Conclusion

Synthetic glasses are a simple way to investigate the effect of different oxides on the reactivity and the resulting compressive strength. For this reason, five different complex slags had been synthesized containing different oxides in addition to the main oxides Al₂O₃, SiO₂ and CaO in amounts equal to an original, commercial slag. In this study, we showed that synthetic slags can exhibit a higher compressive strength compared to the original slag. Differences in compressive strength are partly due to higher

reactivity, which was determined by the R³ test. Differences in reactivity are caused by different degrees of polymerization.

Despite a comparable composition and a similar NBO/T ratio, the original slag achieves a significantly higher total heat than all synthetic slags after 7 days. This increased reactivity cannot be attributed to the structure, as FTIR spectroscopy and ²⁷Al MAS NMR show similarities in the structure. However, ²⁹Si MAS NMR indicates that the calculated degrees of polymerization are realistic, since higher NBO/T ratios lead to a downfield shift, meaning that silicates are less crosslinked.

Overall, it can be concluded that synthetic glasses with a similar NBO/T ratio represent a good approximation to real blast furnace slag and the effects of individual oxides can thus be worked out. Nevertheless, it should be noted that individual components such as crystalline fractions and individual metal oxides, which are present in small quantities, can lead to changes in reactivity and possibly also to slightly different reaction products. To check this, further experiments in cement pastes and in the R³ model system are necessary.

5 Acknowledgments

The research presented is supported by the TUM Georg Nemetschek Institute Artificial Intelligence for the Built World. The authors would like to acknowledge Harald Hilbig and Oksana Storcheva for their help with the NMR spectroscopy and Henrik Eickhoff for the quantification of the mineralogical composition by XRD Rietveld analysis. Additional thanks to the laboratory staff and the student assistants for their help with sample characterization and preparation.

References

- [1] A.K. Hartfield, (2023) *Cement*, in: Mineral commodity summaries 2023, pp. 52–53.
- [2] D.J.M. Flower, J.G. Sanjayan (2007) *Green house gas emissions due to concrete manufacture*, Int J Life Cycle Assess 12, 282–288.
- [3] IEA (2018) *Technology Roadmap: Low-Carbon Transition in the Cement Industry*, Paris.
- [4] A. Favier, C. de Wolf, K.L. Scrivener, G. Habert (2018) *A sustainable future for the European Cement and Concrete Industry: Technology assessment for full decarbonisation of the industry by 2050*, ETH Zurich.
- [5] K.L. Scrivener, V.M. John, E.M. Gartner (2018) *Eco-efficient cements: Potential economically viable solutions for a low-CO₂ cement-based materials industry*, Cement and Concrete Research 114, 2–26.
- [6] D.M. Proctor, K.A. Fehling, E.C. Shay, J.L. Wittenborn, J.J. Green, C. Avent, R.D. Bigham, M. Connolly, B. Lee, T.O. Shepker, M.A. Zak (2000) *Physical and Chemical Characteristics of Blast Furnace, Basic Oxygen Furnace, and Electric Arc Furnace Steel Industry Slags*, Environ. Sci. Technol. 34, 1576–1582.

- [7] D.M. Sadek (2014) *Effect of cooling technique of blast furnace slag on the thermal behavior of solid cement bricks*, Journal of Cleaner Production 79, 134–141.
- [8] H.F.W. Taylor(1990) *Cement chemistry*, Academic Pr, London.
- [9] M.C. Juenger, R. Snellings, S.A. Bernal (2019) *Supplementary cementitious materials: New sources, characterization, and performance insights*, Cement and Concrete Research 122, 257–273.
- [10] E. Lang (2002) *Blastfurnace cements*, in: P. Barnes, J. Bensted (Eds.), *Structure and Performance of Cements*, CRC Press, pp. 310–325.
- [11] R. Snellings, G. Mertens, J. Elsen (2012) *Supplementary Cementitious Materials*, Reviews in Mineralogy and Geochemistry 74, 211–278.
- [12] I.G. Richardson, G.W. Groves (1997) *The structure of the calcium silicate hydrate phases present in hardened pastes of white Portland cement/blast-furnace slag blends*, J Mater Sci 32, 4793–4802.
- [13] E. L'Hôpital, B. Lothenbach, G. Le Saout, D. Kulik, K.L. Scrivener (2015) *Incorporation of aluminium in calcium-silicate-hydrates*, Cement and Concrete Research 75, 91–103.
- [14] M. Ben Haha, B. Lothenbach, G. Le Saout, F. Winnefeld (2012) *Influence of slag chemistry on the hydration of alkali-activated blast-furnace slag — Part II: Effect of Al_2O_3* , Cement and Concrete Research 42, 74–83.
- [15] S.-D. Wang, K.L. Scrivener (1995) *Hydration products of alkali activated slag cement*, Cement and Concrete Research 25, 561–571.
- [16] S.-D. Wang, K.L. Scrivener (2003) *^{29}Si and ^{27}Al NMR study of alkali-activated slag*, Cement and Concrete Research 33, 769–774.
- [17] F. Bellmann, J. Stark (2009) *Activation of blast furnace slag by a new method*, Cement and Concrete Research 3, 644–650.
- [18] S. Teng, T.Y.D. Lim, B. Sabet Divsholi (2013) *Durability and mechanical properties of high strength concrete incorporating ultra fine Ground Granulated Blast-furnace Slag*, Construction and Building Materials 40, 875–881.
- [19] H. Wang, Y. Wang, S. Cui, J. Wang (2019) *Reactivity and Hydration Property of Synthetic Air Quenched Slag with Different Chemical Compositions*, Materials (Basel, Switzerland) 12.
- [20] A. Schöler, F. Winnefeld, M. Ben Haha, B. Lothenbach (2017) *The effect of glass composition on the reactivity of synthetic glasses*, J. Am. Ceram. Soc. 100, 2553–2567.
- [21] DIN Deutsches Institut für Normung e. V., *Prüfverfahren für Zement - Teil 1: Bestimmung der Festigkeit: Deutsche Fassung EN 196-1:2016*, Beuth Verlag GmbH, Berlin 91.100.10 Zement. Gips. Kalk. Mörtel, 2016-11-00.
- [22] F. Avet, R. Snellings, A. Alujas Diaz, M. Ben Haha, K.L. Scrivener (2016) *Development of a new rapid, relevant and reliable (R^3) test method to evaluate the pozzolanic reactivity of calcined kaolinitic clays*, Cement and Concrete Research 85, 1–11.
- [23] C09 Committee, *Standard Test Methods for Measuring the Reactivity of Supplementary Cementitious Materials by Isothermal Calorimetry and Bound Water Measurements*, ASTM International, West Conshohocken, PA.
- [24] P. Lawrence, M. Cyr, E. Ringot (2005) *Mineral admixtures in mortars effect of type, amount and fineness of fine constituents on compressive strength*, Cement and Concrete Research 35, 1092–1105.
- [25] W.A. Gutteridge, J.A. Dalziel (1990) *Filler cement: The effect of the secondary component on the hydration of Portland cement*, Cement and Concrete Research 20, 778–782.
- [26] E. Berodier, K.L. Scrivener (2014) *Understanding the Filler Effect on the Nucleation and Growth of C-S-H*, J. Am. Ceram. Soc. 97, 3764–3773.
- [27] P. Lawrence, M. Cyr, E. Ringot (2003) *Mineral admixtures in mortars: Effect of inert materials on short-term hydration*, Cement and Concrete Research 33, 1939–1947.
- [28] B. Lothenbach, K.L. Scrivener, R.D. Hooton (2011) *Supplementary cementitious materials*, Cement and Concrete Research 41, 1244–1256.
- [29] X. Li, R. Snellings, M. Antoni, N.M. Alderete, M. Ben Haha, S. Bishnoi, Ö. Cizer, M. Cyr, K. De Weerd, Y. Dhandapani, J. Duchesne, J. Haufe, R.D. Hooton, M.C. Juenger, S. Kamali-Bernard, S. Kramar, M. Marroccoli, A.M. Joseph, A. Parashar, C. Patapy, J.L. Provis, S. Sabio, M. Santhanam, L. Steger, T. Sui, A. Telesca, A. Vollpracht, F. Vargas, B. Walkley, F. Winnefeld, G. Ye, M. Zajac, S. Zhang, K.L. Scrivener (2018) *Reactivity tests for supplementary cementitious materials: RILEM TC 267-TRM phase 1*, Mater Struct 51.
- [30] S. Blotevogel, A. Ehrenberg, L. Steger, L. Doussang, J. Kaknics, C. Patapy, M. Cyr (2020) *Ability of the R^3 test to evaluate differences in early age reactivity of 16 industrial ground granulated blast furnace slags (GGBS)*, Cement and Concrete Research 130, 105998.
- [31] Y. Zhang, S. Zhang, Y. Chen, O. Çopuroğlu (2022) *The effect of slag chemistry on the reactivity of synthetic and commercial slags*, Construction and Building Materials 335, 127493.

- [32] C.L. Senior, S. Srinivasachar (1995) *Viscosity of Ash Particles in Combustion Systems for Prediction of Particle Sticking*, Energy Fuels 9, 277–283.
- [33] B.O. Mysen (1983) *The Structure of silicate melts*, Annu. Rev. Earth Planet. Sci. 11, 75–97.
- [34] B.C. Bunker (1994) *Molecular mechanisms for corrosion of silica and silicate glasses*, Journal of Non-Crystalline Solids 179, 300–308.
- [35] S. Rizki Abdila, M. Mustafa Al Bakri Abdullah, M. Faheem Mohd Tahir, R. Ahmad, Syafwandi, M. Isradi (2020) *Characterization of Fly ash and Ground Granulated Blast Slag for Soil Stabilization Application Using Geopolymerization Method*, IOP Conf. Ser.: Mater. Sci. Eng. 864, 12013.
- [36] M. Mollah, W. Yu, R. Schennach, D.L. Cocke (2000) *A Fourier transform infrared spectroscopic investigation of the early hydration of Portland cement and the influence of sodium lignosulfonate*, Cement and Concrete Research 30, 267–273.
- [37] S. Blotevogel, V. Montouillout, A. Canizares, P. Simon, E. Chesneau, A. Danezan, T. Watez, A. Ehrenberg, M. Poirier, C. Patapy, M. Cyr (2021) *Glass structure of industrial ground granulated blast furnace slags (GGBS) investigated by time-resolved Raman and NMR spectroscopies*, J Mater Sci 56, 17490–17504.
- [38] M.J. Toplis, S.C. Kohn, M.E. Smith, I.J. Poplett (2000) *Fivefold-coordinated aluminum in tectosilicate glasses observed by triple quantum MAS NMR*, American Mineralogist 85, 1556–1560.
- [39] G. Engelhardt (1989) *Multinuclear solid-state NMR in silicate and zeolite chemistry*, TrAC Trends in Analytical Chemistry 8, 343–347.
- [40] R. Tänzer, A. Buchwald, D. Stephan (2015) *Effect of slag chemistry on the hydration of alkali-activated blast-furnace slag*, Mater Struct 48, 629–641.